1-1-2014

Hydrostatic piezoelectric properties of [011] poled Pb(Mg 1/3Nb2/3)O3-PbTiO3 single crystals and 2-2 lamellar composites

Lili Li
The Pennsylvania State University, Xian Jiaotong University

Shujun Zhang
The Pennsylvania State University, shujun@uow.edu.au

Zhuo Xu
Xian Jiaotong University

Xuecang Geng
Blatek, Inc.

Fei Wen
Xian Jiaotong University

See next page for additional authors

Hydrostatic piezoelectric properties of [011] poled Pb(Mg 1/3Nb2/3)O3-PbTiO3 single crystals and 2-2 lamellar composites

Abstract

The hydrostatic piezoelectric properties of [011] poled Pb(Mg 1/3Nb2/3)O3-PbTiO3 (PMN-PT) crystals and corresponding 2-2 crystal/epoxy composites were investigated. The crystal volume ratio and compositional dependencies of the hydrostatic charge and voltage coefficients (dh and gh) and hydrostatic figure of merit (FOM) dh x gh were determined, where large FOM value of 3.2 pm2/N with high stability as a function of hydrostatic pressure was achieved for rhombohedral crystal composites. In addition, the stress amplification effects of the face-plate and different epoxy matrixes were investigated, with maximum FOM value being on the order of 92 pm2/N, indicating that 2-2 crystal/epoxy composites are promising materials for hydrostatic applications. 2014 AIP Publishing LLC.

Keywords

pb, poled, 011, properties, piezoelectric, hydrostatic, 2, crystals, single, pbtio3, o3, 3, 3nb2, 1, composites, mg, lamellar

Disciplines

Engineering | Physical Sciences and Mathematics

Publication Details

Li, L., Zhang, S., Xu, Z., Geng, X., Wen, F., Luo, J. & Shrout, T. R. (2014). Hydrostatic piezoelectric properties of [011] poled Pb(Mg 1/3Nb2/3)O3-PbTiO3 single crystals and 2-2 lamellar composites. Applied Physics Letters, 104 (3), 032909-1-032909-5.

Authors

Lili Li, Shujun Zhang, Zhuo Xu, Xuecang Geng, Fei Wen, Jun Luo, and Thomas R. Shrout

AIP | Applied Physics Letters

Hydrostatic piezoelectric properties of [011] poled Pb(Mg1/3Nb2/3)O3-PbTiO3 single crystals and 2-2 lamellar composites

Lili Li, Shujun Zhang, Zhuo Xu, Xuecang Geng, Fei Wen, Jun Luo, and Thomas R. Shrout

Citation: Applied Physics Letters **104**, 032909 (2014); doi: 10.1063/1.4862984
View online: http://dx.doi.org/10.1063/1.4862984
View Table of Contents: http://scitation.aip.org/content/aip/journal/apl/104/3?ver=pdfcov
Published by the AIP Publishing

Hydrostatic piezoelectric properties of [011] poled $Pb(Mg_{1/3}Nb_{2/3})O_3$-$PbTiO_3$ single crystals and 2-2 lamellar composites

Lili Li,[1,2] Shujun Zhang,[1,a)] Zhuo Xu,[2] Xuecang Geng,[3] Fei Wen,[2] Jun Luo,[4] and Thomas R. Shrout[1]
[1]*Materials Research Institute, Pennsylvania State University, University Park, Pennsylvania 16802, USA*
[2]*Electronic Materials Research Laboratory, Key Laboratory of the Ministry of Education, International Center for Dielectric Research, Xi'an Jiaotong University, Xi'an 710049, People's Republic of China*
[3]*Blatek Inc., 2820 E. College Avenue, Suite F, State College, Pennsylvania 16801, USA*
[4]*TRS Technologies Inc., 2820 E. College Avenue, Suite J, State College, Pennsylvania 16801, USA*

(Received 21 December 2013; accepted 9 January 2014; published online 24 January 2014)

The hydrostatic piezoelectric properties of [011] poled $Pb(Mg_{1/3}Nb_{2/3})O_3$-$PbTiO_3$ (PMN-PT) crystals and corresponding 2-2 crystal/epoxy composites were investigated. The crystal volume ratio and compositional dependencies of the hydrostatic charge and voltage coefficients (d_h and g_h) and hydrostatic figure of merit (FOM) $d_h \times g_h$ were determined, where large FOM value of 3.2 pm^2/N with high stability as a function of hydrostatic pressure was achieved for rhombohedral crystal composites. In addition, the stress amplification effects of the face-plate and different epoxy matrixes were investigated, with maximum FOM value being on the order of 92 pm^2/N, indicating that 2-2 crystal/epoxy composites are promising materials for hydrostatic applications.
 [http://dx.doi.org/10.1063/1.4862984]

Piezoelectric materials are of particular interest owing to their outstanding performance in converting mechanical signals to electrical signals and vice versa. Lead zirconate titanate (PZT) ceramics and relaxor-$PbTiO_3$ (PT) crystals with morphotropic phase boundary (MPB) compositions possess high-piezoelectric coefficients and are technologically important for various electromechanical applications.[1–3] For piezoelectric sensors, they offer advantages of high reliability, fast response time, insensitivity to electrical and magnetic fields, and thus have been widely used for measuring force, strain, pressure, acceleration, to name a few.[4] Hydrophone is one important category of piezoelectric sensors, which detects the pressure variation of acoustic signals in water, while producing an output voltage proportional to the pressure.[5–8] The acoustic pressure is considered to be effectively hydrostatic as the wavelengths of sounds in low frequency range are much larger than the sensor dimensions. The voltage produced under hydrostatic pressure is used to measure the sensitivity of a hydrophone. In this regard, a useful parameter in evaluating piezoelectric materials for use in hydrophones is the voltage coefficient g_h. Another parameter is the hydrostatic charge coefficient d_h, which describes polarization resulting from a change in stress, with $d_h = d_{33} + d_{31} + d_{32}$ (for poled polycrystalline ceramics, $d_{31} = d_{32}$). Here, d_{33} and d_{31}/d_{32} are the longitudinal and transverse coefficients, respectively. A useful figure of merit (FOM) for hydrophone materials is the product of the voltage and charge coefficients, $d_h \times g_h$.[9] A basic limitation on hydrophone performance is the electrical noise generated internally, which must not exceed the total sea noise.[7] At frequencies far below the resonance frequency, the energy dissipation is mainly dominated by the dielectric loss, thus the alternative FOM ($d_h \times g_h/\tan\delta$) has been proposed.[7,10] Other desirable properties for hydrophone sensors include, but are not limited to, low density for good acoustic impedance matching with water, minimal variation of d_h and g_h with pressure and temperature, etc.[6]

PZT ceramics and relaxor-PT single crystals have been widely used for transducer applications; however, they have limited utility in transducers under hydrostatic conditions because of their relatively low hydrostatic piezoelectric coefficients, due to the fact that the d_{33} is about twice the magnitude and opposite in sign from d_{31}, thus leading to relatively low d_h. In addition, the high permittivity results in low g_h coefficients. There has been a longtime interest in developing piezoelectric composites for hydrophone applications, because of their high hydrostatic sensitivity, good acoustic impedance matching to water, and high-pressure tolerance.[11–26] Piezocomposite hydrophones are dominated by 1-3 type connectivity, in which the arrangement of piezoelectric material and polymer will reduce the influence of the 31 and 32 modes and produce a significant improvement in hydrostatic voltage sensitivity, with a high FOM.[11–20] Other engineered connectivities, such as parallel-connected 2–2 composites, which are stacks of piezoelectric ceramic sheets separated by passive polymer layers, have also been investigated.[21–26] Recently, 2-2 lamellar composites comprised of relaxor-PT single crystals have been studied, giving a promising FOM of 16 pm^2/N for a crystal volume of 25%.[27,28] The 2-2 composite takes advantage of the strong anisotropic behavior of $[011]_C$ poled single crystals, with macroscopic mm2 symmetry, in which the d_{33} and d_{31} are both positive, while d_{32} is negative. The contribution of d_{32} to the hydrostatic d_h value is greatly reduced when the polymer layers are perpendicular to the 2 direction (Y axis, as shown in Fig. 1, where the $[011]_C$ direction is along Z axis, while $[0\bar{1}1]_C$ and $[100]_C$ are the X and Y axes, respectively), with minimal reduction of the d_{33} and d_{31} values, thus, the hydrostatic piezoelectric d_h is significantly improved.[2] The theoretical results reported, however, have yet

a)Author to whom correspondence should be addressed. Electronic mail: soz1@psu.edu

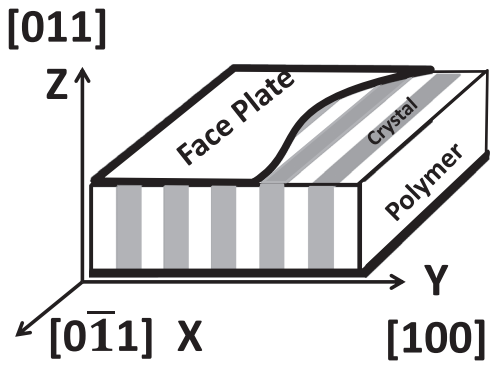

FIG. 1. Schematic diagram of 2-2 crystal/epoxy composite comprised of [011] poled PMN-PT crystals, with layers parallel to *X* axes.

to be experimentally confirmed, which is the topic of this research.

In this paper, $[011]_C$ poled monolithic $Pb(Mg_{1/3}Nb_{2/3})O_3$-$PbTiO_3$ (PMN-PT) crystals and corresponding 2-2 composites with various compositions were fabricated, the quasi-static measurements[29] were taken to determine the hydrostatic properties. In addition, the face-plate and epoxy matrixes (with different Young's moduli and Poisson's ratios) were investigated to further improve the hydrostatic piezoelectric properties.

PMN-PT single crystals were grown using Bridgman method at TRS Technologies Inc. Single crystals with rhombohedral (R) and orthorhombic (O) phases were selected for study. All samples were oriented using a real time Laue X-ray system with an accuracy of $\pm 0.5°$ along the $\langle 100\rangle_C$ and $\langle 011\rangle_C$ crystallographic directions. The 2-2 crystal/epoxy composites with various PMN-PT volume ratios were fabricated using the conventional dice and fill method, where the dicing was along the $[0\bar{1}1]_C$ direction of the single crystals. The kerf width was controlled to be 0.35 mm, with crystal sheet width being 0.58–1.0 mm, leading to 40%–66% crystal volume ratios. The epoxies [Epoheat (Buehler), Epoheat/DER732-75/25 wt.% (DOW Chemical) and Epoheat/DER732 with 10% volume of Matsumoto microsphere MFL-80GCA] with 25 wt. % hardener were then backfilled into the grooves in vacuum for 30 min, and subsequently cured at 20–80 °C. The fabricated composites were polished until all the piezoelectric sheets were exposed, and the final dimensions were $10 \times 10 \times 1.0 \sim 1.5$ mm^3. All the samples were sputtered with gold electrodes on the $(011)_C$ surfaces, and poled with a field of 10–15 kV/cm at room temperature. For face-plate composites, the copper plates with 0.3 mm thickness were affixed to the composite using conductive epoxy (E-Solder 3022). The dielectric properties of the prepared monolithic and composite samples were determined using an HP4184A LCR meter. The piezoelectric hydrostatic coefficient d_h was determined by the quasi-static method, following the formula:[30]

$$\frac{\Delta Q}{A} = \left[d_h + \frac{1}{2}a_1(p - p_0)\right] \cdot (p - p_0), \tag{1}$$

where Q is the charge created on the sample, A is the value of the electrode area, d_h is the hydrostatic piezoelectric charge coefficient at room temperature and atmosphere pressure, and p_0 is atmospheric pressure. a_1 is the isothermal pressure coefficient, being used to evaluate the pressure stability of d_h with the following formula:

$$d_h(p) = d_h + a_1 \times (p - p_0). \tag{2}$$

Another normalized pressure coefficient, $\frac{a_1}{d_h}$, in ppm/Pa, was also used in this research for comparison purpose.

Table I summarizes the measured dielectric and hydrostatic piezoelectric properties of [011] poled PMN-PT crystals. The PMN-PT samples were numbered (#1 to #6) in ascending order from the bottom of the crystal boule, exhibiting rhombohedral (R) and orthorhombic (O) phases, respectively. The d_{33} values and relative dielectric permittivity of the R crystals increase from 1180 to 1850 pC/N and 3730 to 5920, respectively, from samples #1 to #4, while the values are about 320–300 pC/N and 1180–1120 for samples #5 and #6, due to the fact that [011] poled O crystals possess single domain state, accounts for the very low dielectric/piezoelectric properties.[31] The pressure dependence of the measured charge density for [011] poled PMN-PT crystals as a function of applied pressure, up to 200 MPa, is presented in Fig. 2. The experimental data was fitted using Eq. (1), where the hydrostatic piezoelectric d_h and pressure coefficient a_1 (or $\frac{a_1}{d_h}$) were determined and summarized in Table I. It should be noted that the hydrostatic piezoelectric d_h values for [011] poled PMN-PT with different compositions and phases were found to be on the order of 70 to 90 pC/N, significantly smaller than d_h values calculated from the longitudinal piezoelectric d_{33}, transverse piezoelectric d_{31} (positive) and d_{32} (negative), which are generally about 150–300 pC/N.[32–36] The large differences of d_h values in O phase crystals are due to the instability of the single domain state, which can be confirmed by the single domain piezoelectric coefficients obtained under *dc* bias field.[32,33] Of interest is that the calculated d_h values of Mn:$Pb(In_{0.5}Nb_{0.5})O_3$-PMN-PT (Mn:PIN-PMN-PT) crystals were found to be on the order of 75 pC/N, very close to the experimentally determined values, due to the stabilized single domain state

TABLE I. Dielectric/piezoelectric properties of [011] poled PMN-PT crystals for various compositions and phases.

Sample	ε_r	Loss (%)	d_{33} (pC/N)	d_h (pC/N)	g_h (mVm/N)	FOM (pm^2/N)	$\frac{a_1}{d_h}$ (ppm/Pa)
R (1)	3730	0.3	1180	70	2.1	0.15	0.001
R (2)	4590	0.3	1280	80	2.0	0.16	0.0013
R (3)	5130	0.5	1600	80	1.8	0.14	0.001
R (4)	5920	0.5	1850	80	1.5	0.12	0.0011
O (5)	1180	0.4	320	90	8.6	0.78	0.0016
O (6)	1120	0.5	300	70	7.1	0.50	0.001

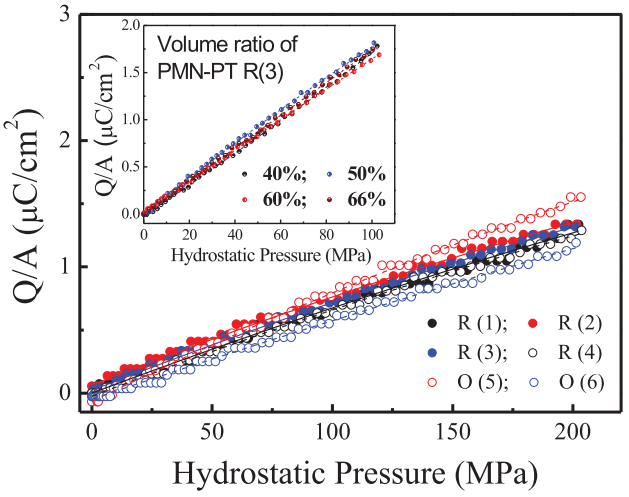

FIG. 2. The hydrostatic pressure dependence of the charge density for [011] poled crystals with various compositions and phases, small inset shows the pressure dependence of the charge density for 2-2 composites with various PMN-PT volume ratios.

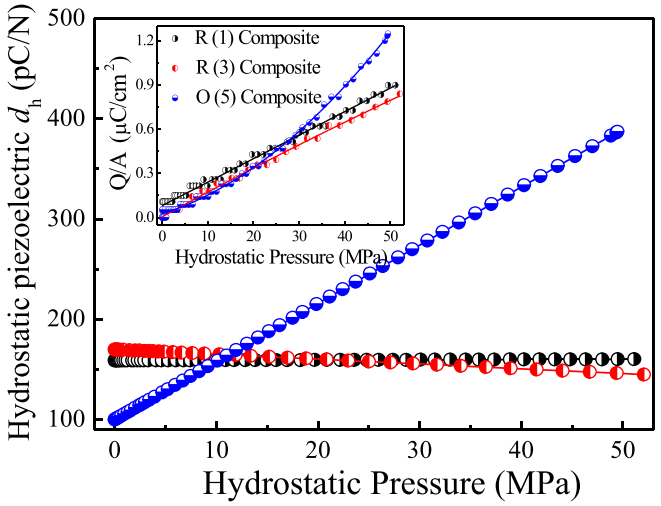

FIG. 4. The hydrostatic pressure dependence of d_h for 2-2 composites with various composition and phases, the small inset shows the hydrostatic pressure dependence of the charge density for 2-2 composites with various composition and phases.

by the existence of internal bias.[37] On the contrary, the large differences between the calculated and measured d_h values in R crystals, maybe owing to the domain engineered configurations, other than the extrinsic contribution.[32,33] The hydrostatic piezoelectric g_h and FOM of O crystals reached 8.6 mVm/N and 0.78 pm^2/N, respectively, which are much higher than those of the R crystals (2.0 mVm/N and 0.16 pm^2/N), due to their low relative dielectric permittivity (~1200). Of importance is that all the crystal samples exhibit very low isothermal pressure coefficient, with $\frac{a_1}{d_h}$ being on the order of 0.001 ppm/Pa, demonstrating minimal variation as a function of hydrostatic pressure.

The pressure dependence of the charge density for 2-2 crystal/epoxy lamellar composites with different PMN-PT volume ratios is given in the small inset of Figure 2 [the R (3) composition was selected for crystal component, while Epoheat resin was selected as the epoxy]. The coefficients d_h/g_h and FOM were calculated and given in Fig. 3. The d_h was found to be relatively insensitive to the volume ratio of PMN-PT ($V_{\text{PMN-PT}}$), with values being in the range of 160–200 pC/N, while the g_h (from 6.0 to 20 mVm/N) and FOM (1.1 to 3.2 pm^2/N) decreased almost linearly with the increasing of $V_{\text{PMN-PT}}$ due to the increase of dielectric

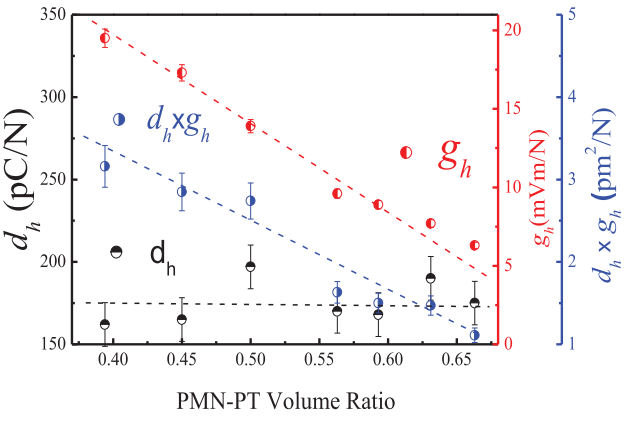

FIG. 3. The hydrostatic properties of 2-2 crystal/epoxy composites as a function of PMN-PT volume ratios.

permittivity. The hydrostatic coefficient d_h and the pressure induced charge density for the 2-2 composites (40–50 vol. % ratio) with R (1), R (3), and O (5) PMN-PT crystals were measured as a function of applied hydrostatic pressure up to 50 MPa, as given in Fig. 4 and the small inset, respectively. The dielectric and piezoelectric properties are summarized in Table II. It was found that the R (3) composite exhibited the highest relative dielectric permittivity ~2300, while the O (5) composite possessed the lowest properties inherently associated with the single domain state. The piezoelectric coefficients d_h and g_h, FOM and normalized pressure coefficient $\frac{a_1}{d_h}$ of the 2-2 composites are also listed in the table. R (1) and R (3) composites were found to possess similar d_h values, being around 160–180 pC/N. However, R (1) composite exhibited higher g_h (12.0 mVm/N) and FOM (1.90 pm^2/N) than those values of R (3) composite, as a result of the lower dielectric permittivity. Though the charge coefficient of O (5) crystal/epoxy composite is much lower than its R counterparts, the FOM is higher, due to the low dielectric permittivity. Of particular significance is that the R (1) composites show very low normalized pressure coefficients, being only 0.0002 ppm/Pa, one order magnitude lower than R (3) and more than two orders magnitude lower than O (5) composites. This is due to the fact that R (1) composition is in rhombohedral phase, being far away from the MPB composition. Furthermore, it was observed both R crystals exhibit minimal pressure variation, as given in Fig. 4, indicating very high hydrostatic pressure stability, while O crystals possess inferior pressure dependent

TABLE II. Dielectric/piezoelectric properties of 2-2 composites with various compositions and phases.

Samples	ε_r	Loss (%)	d_h (pC/N)	g_h (mVm/N)	FOM (pm^2/N)	$\frac{a_1}{d_h}$ (ppm/Pa)
R (1) composite	1500	1.0	160	12	1.9	0.0002
R (3) composite	2300	1.0	180	7.8	1.4	−0.003
O (5) composite	470	1.0	100	24	2.4	0.06

TABLE III. Dielectric/piezoelectric properties of face-plate stabilized 2-2 composites with various matrixes.

Samples	ε_r	Loss (%)	d_h (pC/N)	g_h (mVm/N)	FOM (pm^2/N)	$\frac{a_1}{d_h}$ (ppm/Pa)
R (1)-hard	1500	1.0	190	14.5	2.7	0.005
R (1)-soft	1550	1.0	250	18.2	4.6	0.015
R (1)-soft + bubbles	1500	1.0	390	29.4	11	0.016
O (5)-hard	470	1.0	170	40.9	6.9	0.067
O (5)-soft	460	1.0	380	94.3	35	0.034
O (5)-soft + bubbles	400	1.0	570	161	92	0.031

behavior, which may be associated with the hydrostatic pressure induced flattening of the free-energy profile along the polar axis in single domain O crystals.[38]

For piezocomposites, including 1-3, 1-1-3, 2-2 ceramic/epoxy composites, lot of attentions have been focused on the axial stress amplification and lateral stress attenuation by adding face-plate, changing the matrix stiffness and Poisson's ratio, which will greatly increase the hydrostatic charge coefficient.[21–26] The effects of copper face-plate, matrix stiffness and Poisson's ratio on the 2-2 crystal/epoxy composites were also investigated in this work and the results are given in Table III and Fig. 5, where R (1)-hard means the composite fabricated by PMN-PT crystal with R (1) composition and Epoheat resin (stiff epoxy with high Young's modulus), while O (5)-soft is the composite prepared by PMN-PT crystal with O (5) composition and Epoheat/DER732 (75/25) resin (soft epoxy with low Young's modulus). The soft + bubbles is the low Poisson's ratio epoxy. It was found that the coefficient d_h for R (1) composite increased from 160 pC/N to 190 pC/N with copper face-plate, while the O (5) composite increased from 100 pC/N to 170 pC/N (as shown in Tables II and III), due to the fact that the additional stress transfers between the two constituents via the face-plate is primarily a normal stress along the *Z*-axis, thus amplifying the axial pressure and giving rise to higher hydrostatic properties.[23,24,39] Certainly, the amplification effect in a face-plated composite also depends on the thickness and stiffness of the face-plate, which was not studied here. The d_h was further increased to 250 pC/N and 380 pC/N for R (1)-soft and O (5)-soft based 2-2 composites, respectively, as listed in Table III. This phenomenon is due to the softer polymer matrix with decreased Young's modulus, which leads to axial stress amplification, account for the improved hydrostatic properties.[21–23] In addition, with the face-plate, composites made of softer polymer (low Young's modulus) will have more uniform displacement than composites made of harder polymer (high Young's modulus), due to the fact that the additional stress transferred by the face-plate from the crystal to the polymer is in the form of a normal stress, where the softer polymer has less resistance to elastic deformation, thus it is easier to be driven toward more uniform displacement of the crystal sheets with the help of face-plates.[24] The Poisson's ratio of the polymer matrix is also a very important parameter in designing piezocomposites for hydrostatic applications. If the Poisson's ratio of the polymer matrix is large, the polymer matrix will be hydrostatically incompressible and large lateral stresses will develop in the piezoelectric crystals.[21] The Poisson's ratios for most polymers are 0.35–0.4, which can be reduced by introducing the bubbles into the polymer matrix.[40,41] Ten volume percent microsphere MFL-80GCA with 10–30 μm diameter was introduced into polymer matrix, as expected, the d_h values were found to increase to 390 pC/N and 570 pC/N for R (1)-soft + bubbles and O (5)-soft + bubbles composites, respectively, with the FOM values being on the order of 11 pm^2/N and 92 pm^2/N, considerably higher than those values of 2-2 composites with stiff and high Poisson's ratio epoxy. The pressure dependent hydrostatic charge coefficients were given in Fig. 5, the normalized pressure coefficients were also listed in Table III, where one can see that the face-plate will slightly deteriorate pressure stability of the hydrostatic properties, due to the stress amplification effect of the face-plate. Of particular significance is that the bubbles mixed epoxy matrix with decreased Poisson's ratio showed similar normalized pressure coefficient as that of the soft epoxy, but with much higher hydrostatic FOM values.

Table IV gives the comparison of the hydrostatic properties for various piezoelectric materials, including polymer, ceramics, crystals, and composites. [011] poled PMN-PT

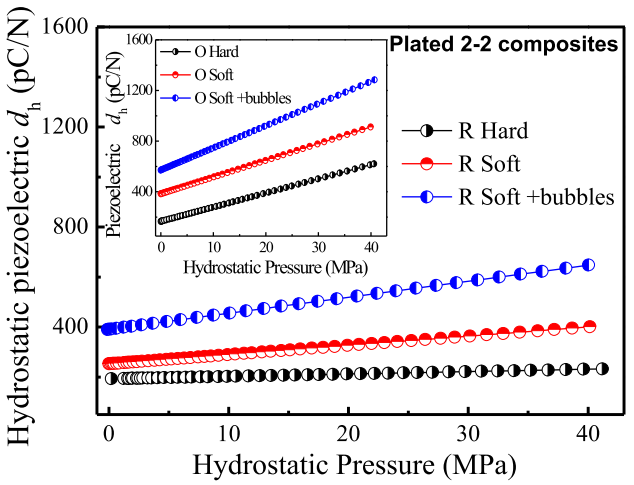

FIG. 5. The hydrostatic pressure dependence of d_h for face-plate stabilized 2-2 composites with various epoxy matrixes.

TABLE IV. Comparison of hydrostatic properties for various materials.

Material	ε_r	d_h (pC/N)	g_h (mVm/N)	FOM (pm^2/N)
PVDF polymer[a]	13	6	53	0.32
$PbNb_2O_6$ ceramic[a]	225	67	34	2.3
PZT ceramic[a]	1800	40	2.5	0.10
[100] PMN-PT crystal[a]	4436	80	2	0.16
[011] PIN-PMN-PT "2R"[a]	3000	87	3	0.29
[011] PIN-PMN-PT "1O"[a]	1500	110	8	0.91
PZT 0-3 composite[a]	100	28	32	0.90
PZT 1-3 composite[a]	200	78	40	3.1
[011] R(1) composite[b]	1500	160	12	1.9
[011] O(5) composite[b]	470	100	24	2.4
[011] R (1)-soft + bubbles[b]	1500	390	29	11
[011] O (5)-soft + bubbles[b]	400	570	161	92

[a]References 2, 3, 13, and 27.
[b]This work.

crystals offer high d_h, but the high permittivity leads to low g_h and FOM. Of particular interest is that the 2-2 crystal/epoxy composites comprised of [011] poled relaxor-PT crystals, with the lamellar direction parallel to X axes, show increased hydrostatic properties, due to the fact that the large negative d_{32} coefficients are greatly eliminated in this structure. In addition, the hydrostatic properties of the 2-2 composites were found to be significantly enhanced by adding stiff face-plate, decreasing the Young's modulus and Poisson's ratio of the epoxy matrix. The highest FOM value, being on the order of 92 pm^2/N, was achieved for O (5)-soft + bubbles 2-2 composites, with $\frac{d_3}{d_h}$ being on the order of 0.031 ppm/Pa, while R (1)-soft + bubbles 2-2 composite was found to possess FOM value of 11 pm^2/N, with much higher pressure stability. The large hydrostatic piezoelectric properties, together with optimized composite structure, will make the 2-2 lamellar composites promising for hydrostatic transducer applications.

This work was supported by ONR and NIH under 2P41EB002182-15A1.O. The authors from XJTU acknowledge National Nature Science Foundation of China (Grant Nos. 51102193 and 51002116).

[1]S. E. Park and T. R. Shrout, J. Appl. Phys. **82**, 1804 (1997).
[2]S. J. Zhang and F. Li, J. Appl. Phys. **111**, 031301 (2012).
[3]Z. G. Ye, *Handbook of Advanced Dielectric, Piezoelectric and Ferroelectric Materials- Synthesis, Characterization and Applications* (Woodhead, Cambridge, England, 2008).
[4]X. N. Jiang, K. R. Kim, S. Zhang, J. Johnson, and G. Salazar, Sensors **14**, 144 (2014).
[5]J. F. Tressler, S. Alkoy, and R. E. Newnham, J. Electroceram. **2**, 257 (1998).
[6]E. K. Akdogan, M. Allahverdi, and A. Safari, IEEE Trans. Ultrason. Ferroelect. Freq. Control **52**, 746 (2005).
[7]C. H. Sherman and J. L. Butler, *Transducers and Arrays for Underwater Sound* (Springer, NY, 2007).
[8]H. Li, Z. D. Deng, and T. J. Carlson, Sens. Lett. **10**, 679 (2012).
[9]A. Safari, Y. Lee, A. Halliyal, and R. Newnham, Am. Ceram. Soc. Bull. **66**, 668 (1987).
[10]A. S. Bhalla and R. Y. Ting, Sens. Mater. **4**, 181 (1988).
[11]W. A. Smith, IEEE Trans. Ultrason. Ferroelect. Freq. Control **40**, 41 (1993).
[12]W. A. Smith, A. A. Shaulov, and B. A. Auld, Ferroelectrics **91**, 155 (1989).
[13]R. E. Newnham, L. J. Bowen, K. A. Klicker, and L. E. Cross, Mater. Des. **2**, 93 (1980).
[14]K. A. Klicker, J. V. Biggers, and R. E. Newnham, J. Am. Ceram. Soc. **64**, 5 (1981).
[15]R. E. Newnham, A. Safari, J. Giniewicz, and B. H. Fox, Ferroelectrics **60**, 15 (1984).
[16]A. Safari, A. Halliyal, L. Bowen, and R. Newnham, J. Am. Ceram. Soc. **65**, 207 (1982).
[17]X. Jiang, J. R. Yuan, A. Cheng, P. Cao, K. Snook, and W. Hackenberger, in *2006 IEEE Ultrasonics Symposium* (2006), pp. 922–925.
[18]X. N. Jiang, P. W. Rehrig, W. S. Hackenberger, E. Smith, S. X. Dong, D. Viehland, J. Moore, and B. Patrick, Proc. SPIE **5761**, 253–262 (2005).
[19]S. J. Zhang, F. Li, J. Luo, R. Sahul, and T. R. Shrout, IEEE Trans. Ultrason. Ferroelect. Freq. Control **60**, 1572 (2013).
[20]W. A. Smith, Proc. SPIE **1733**, 3–26 (1992).
[21]L. Li and N. R. Sottos, J. Appl. Phys. **77**, 4595 (1995).
[22]L. Li and N. R. Sottos, Ferroelectr. Lett. **21**, 41 (1996).
[23]Q. M. Zhang, J. Chen, H. Wang, J. Zhao, L. E. Cross, and M. C. Trottier, IEEE Trans. Ultrason. Ferroelect. Freq. Control **42**, 774 (1995).
[24]W. W. Cao, Q. M. Zhang, J. Z. Zhao, and L. E. Cross, IEEE Trans. Ultrason. Ferroelect. Freq. Control **42**, 37 (1995).
[25]X. Geng and Q. M. Zhang, Appl. Phys. Lett. **67**, 3093 (1995).
[26]X. Geng and Q. Zhang, IEEE Trans. Ultrason. Ferroelect. Freq. Control **44**, 857 (1997).
[27]V. Y. Topolov, A. V. Krivoruchko, C. R. Bowen, and A. A. Panich, Ferroelectrics **400**, 410 (2010).
[28]V. Y. Topolov, C. R. Bowen, and A. V. Krivoruchko, Ferroelectrics **444**, 84 (2013).
[29]J. J. Gao, Z. Xu, F. Li, C. H. Zhang, Y. Liu, G. M. Liu, and H. L. He, J. Adv. Dielectr. **2**, 1250018 (2012).
[30]L. Burianova, P. Hana, S. Panos, J. Kulek, and Y. Tyagur, Ferroelectrics **241**, 59 (2000).
[31]F. Li, S. Zhang, Z. Xu, X. Wei, J. Luo, and T. Shrout, J. Appl. Phys. **108**, 034106 (2010).
[32]S. Liu, S. E. Park, H. Lei, L. E. Cross, and T. R. Shrout, Ferroelectrics **221**, 169 (1999).
[33]S. F. Liu, S. E. Park, T. R. Shrout, and L. E. Cross, J. Appl. Phys. **85**, 2810 (1999).
[34]P. Hana, L. Burianova, E. Furman, S. J. Zhang, T. R. Shrout, and L. E. Cross, Integr. Ferroelectr. **63**, 63 (2004).
[35]L. Burianova, P. Hana, S. Panos, E. Furman, S. J. Zhang, and T. R. Shrout, J. Electroceram. **13**, 443 (2004).
[36]E. Sun, S. Zhang, J. Luo, T. Shrout, and W. Cao, Appl. Phys. Lett. **97**, 032902 (2010).
[37]X. Q. Huo, S. J. Zhang, G. Liu, R. Zhang, J. Luo, R. Sahul, W. Cao, and T. R. Shrout, J. Appl. Phys. **112**, 124113 (2012).
[38]J. J. Gao, Z. Xu, F. Li, C. H. Zhang, Y. Liu, G. M. Liu, and H. L. He, J. Appl. Phys. **109**, 114111 (2011).
[39]W. Cao, Q. Zhang, and L. Cross, IEEE Trans. Ultrason. Ferroelect. Freq. Control **40**, 103 (1993).
[40]M. J. Haun and R. E. Newnham, Ferroelectrics **68**, 123 (1986).
[41]W. A. Smith, in *1991 IEEE Ultrasonics Symposium* (1991), pp. 661–665.